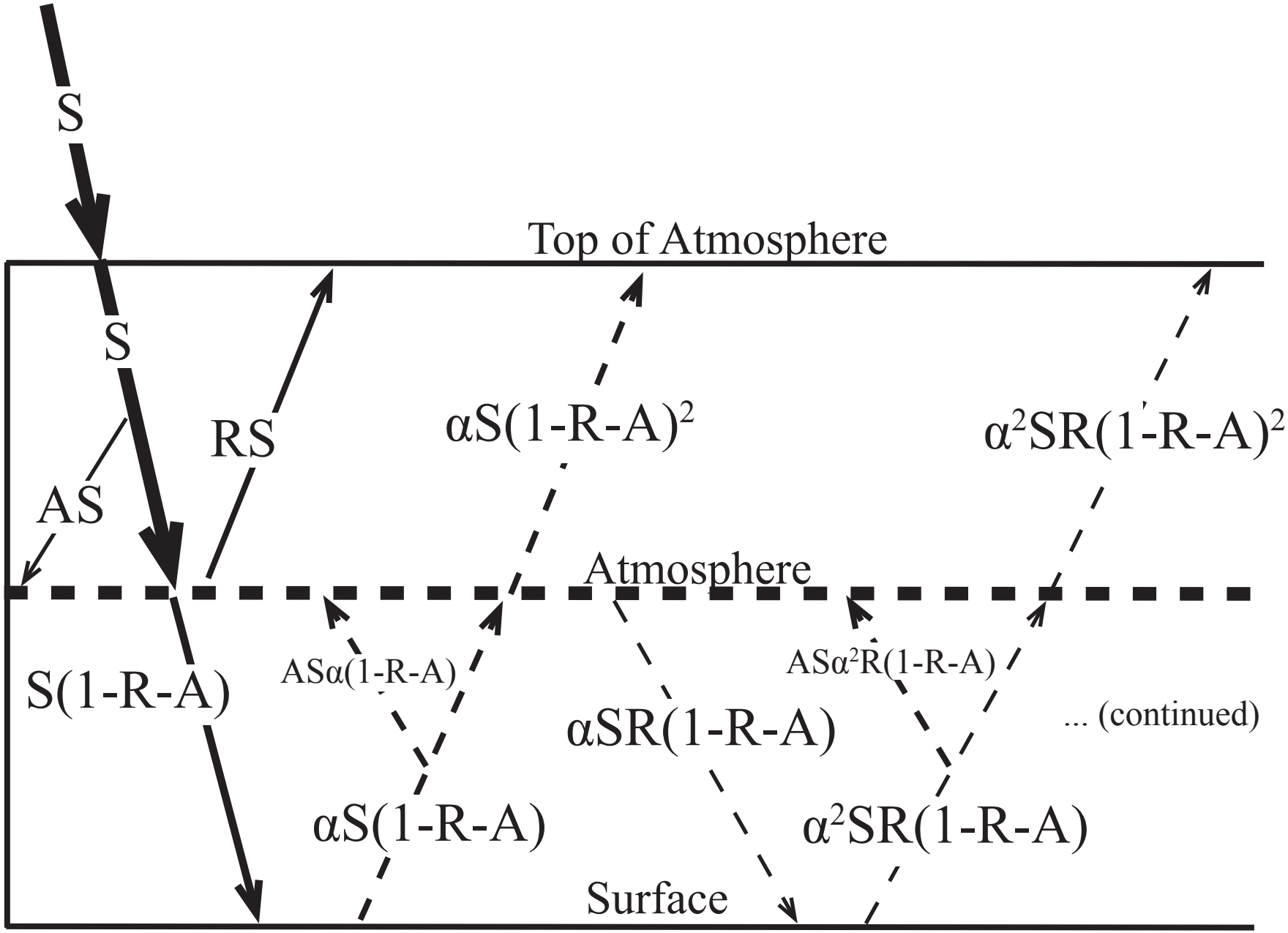

FIG 1. Schematic representing the first two reflections in the single layer solar radiation model. Moving from left to right, the arrows represent the radiative fluxes associated with the incident solar, first reflection, and second reflection. A, R, and α are the atmospheric absorption fraction during a single pass through the atmosphere, the fraction of cloud reflection, and the surface albedo respectively. The solid (dashed) arrows at the TOA represent the radiative fluxes we associated with cloud (surface) reflection.

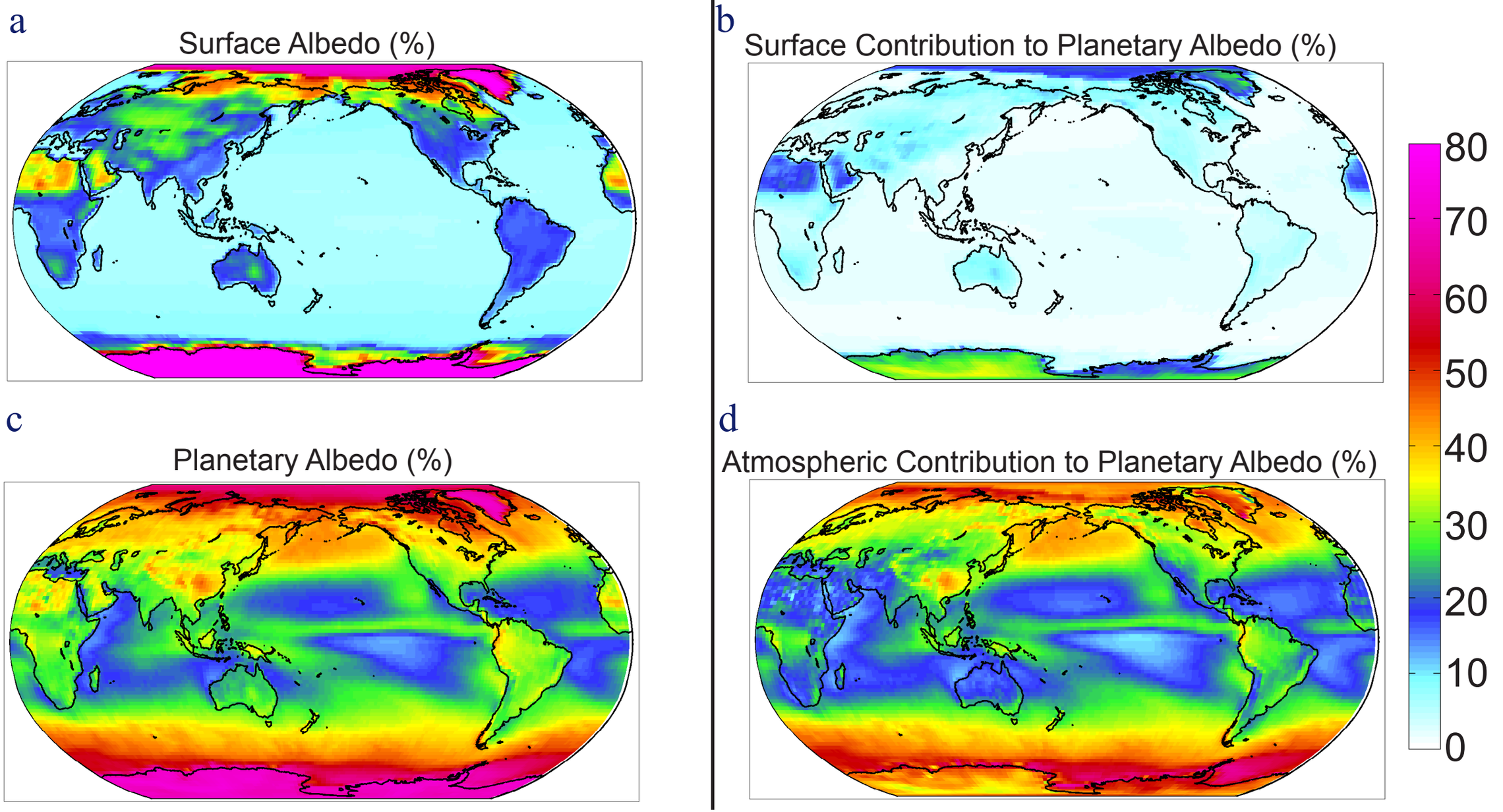

FIG 2. (a and c) The surface albedo and planetary albedo, expressed as a percent. (b and d) $\alpha_{P,SURF}$ and $\alpha_{P,ATMOS}$ expressed as a percent.

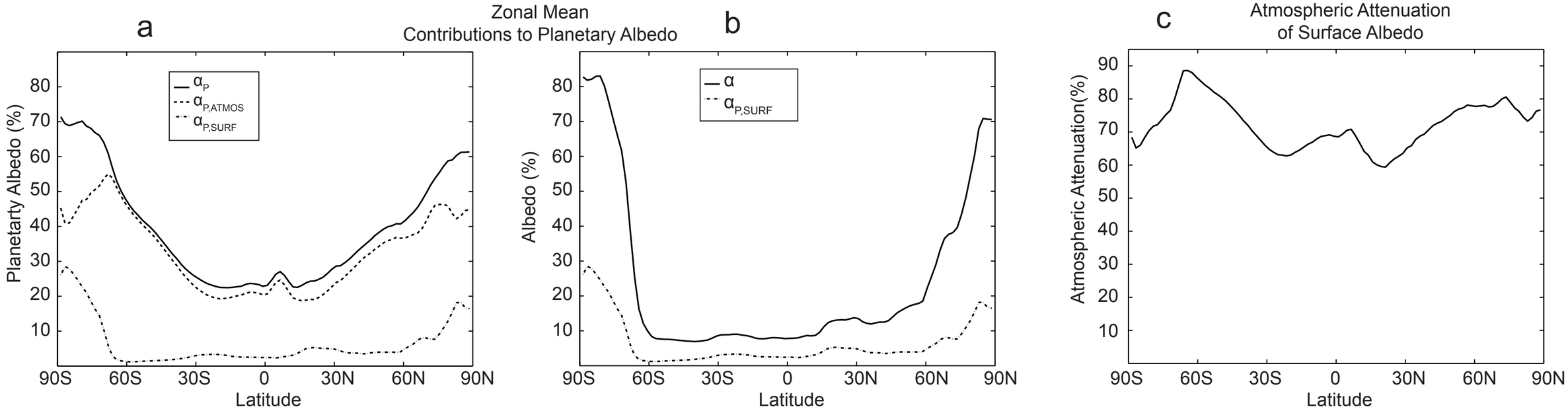

FIG 3. (a) Zonal mean planetary albedo partitioned between atmospheric and surface components. (b) Zonal mean surface albedo and $\alpha_{P,SURF}$. (c) Atmospheric attenuation of surface albedo.

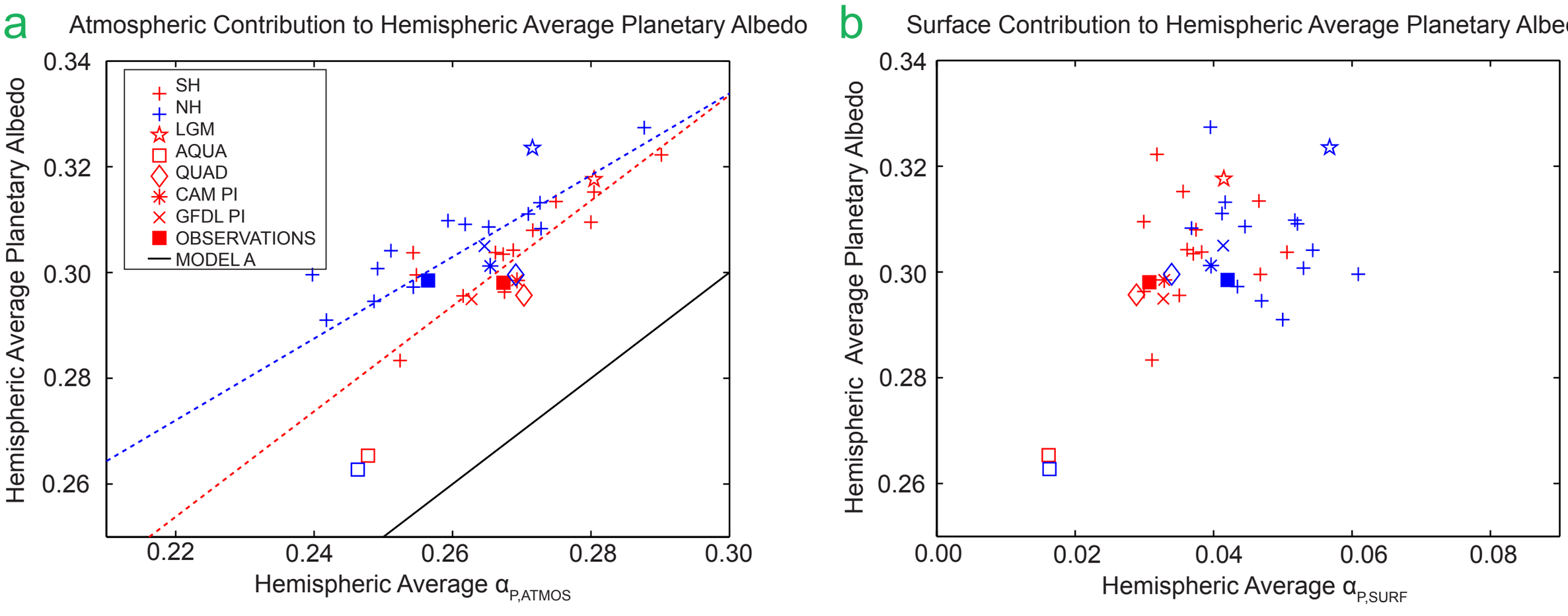

FIG4. (a) Hemispheric average planetary albedo versus hemispheric average $\alpha_{P,ATMOS}$ in the CMIP3 PI simulations (crosses), observations (filled squares), and altered climate states . Red symbols and lines are for the Southern Hemisphere (SH) while blue denotes the Northern Hemisphere (NH). The dashed lines are linear best fits to the PI simulations and the solid line is the 1:1 line with zero intercept. (b) as in (a) except plotted against hemispheric average $\alpha_{P,SURF}$.

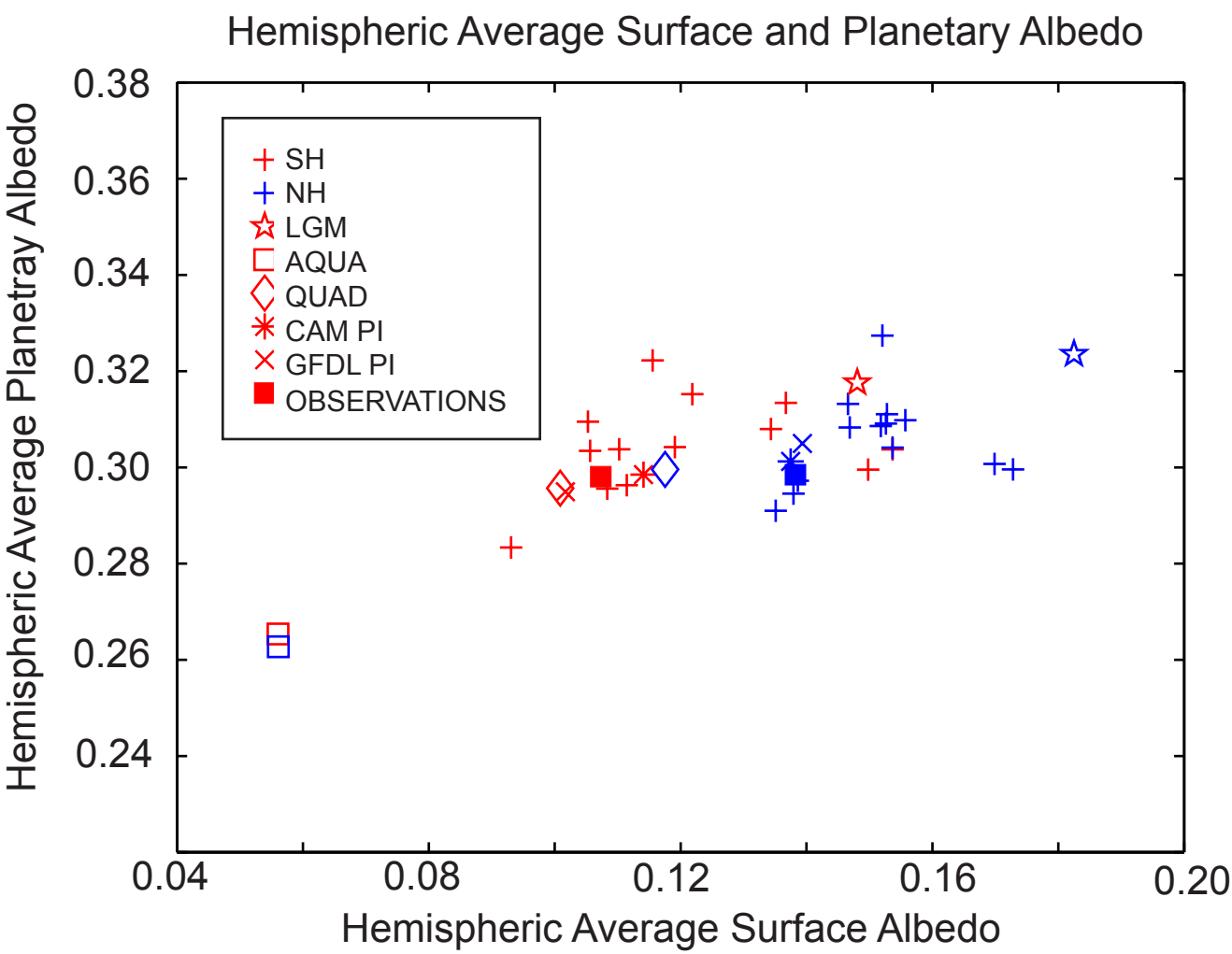

FIG 5. Hemispheric average planetary albedo versus hemispheric average surface albedo in the PI CMIP3 simulation (crosses), observations (filled squares), and altered climate states. Red symbols and lines are for the Southern Hemisphere (SH) while blue denotes the Northern Hemisphere (NH). The axes have a 1:1 ratio.

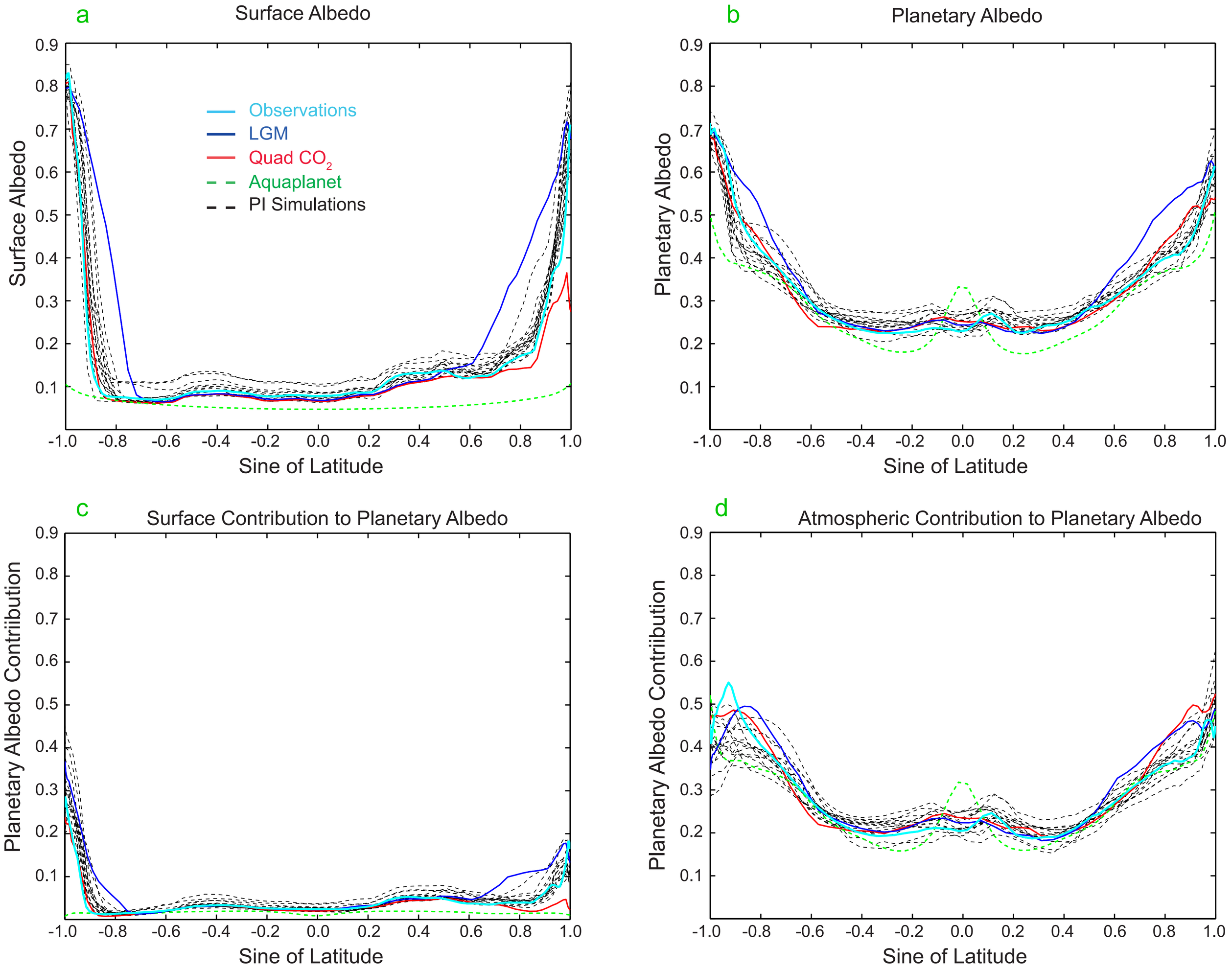

FIG 6. Zonal annual mean (a) surface albedo, (b) planetary albedo, (c) $\alpha_{P,SURF}$ and (d) $\alpha_{P,ATMOS}$ in the PI simulations from the CMIP3 models (dashed black lines). Also shown are the observations (solid, light blue) and model simulations of altered climate states (colored lines).

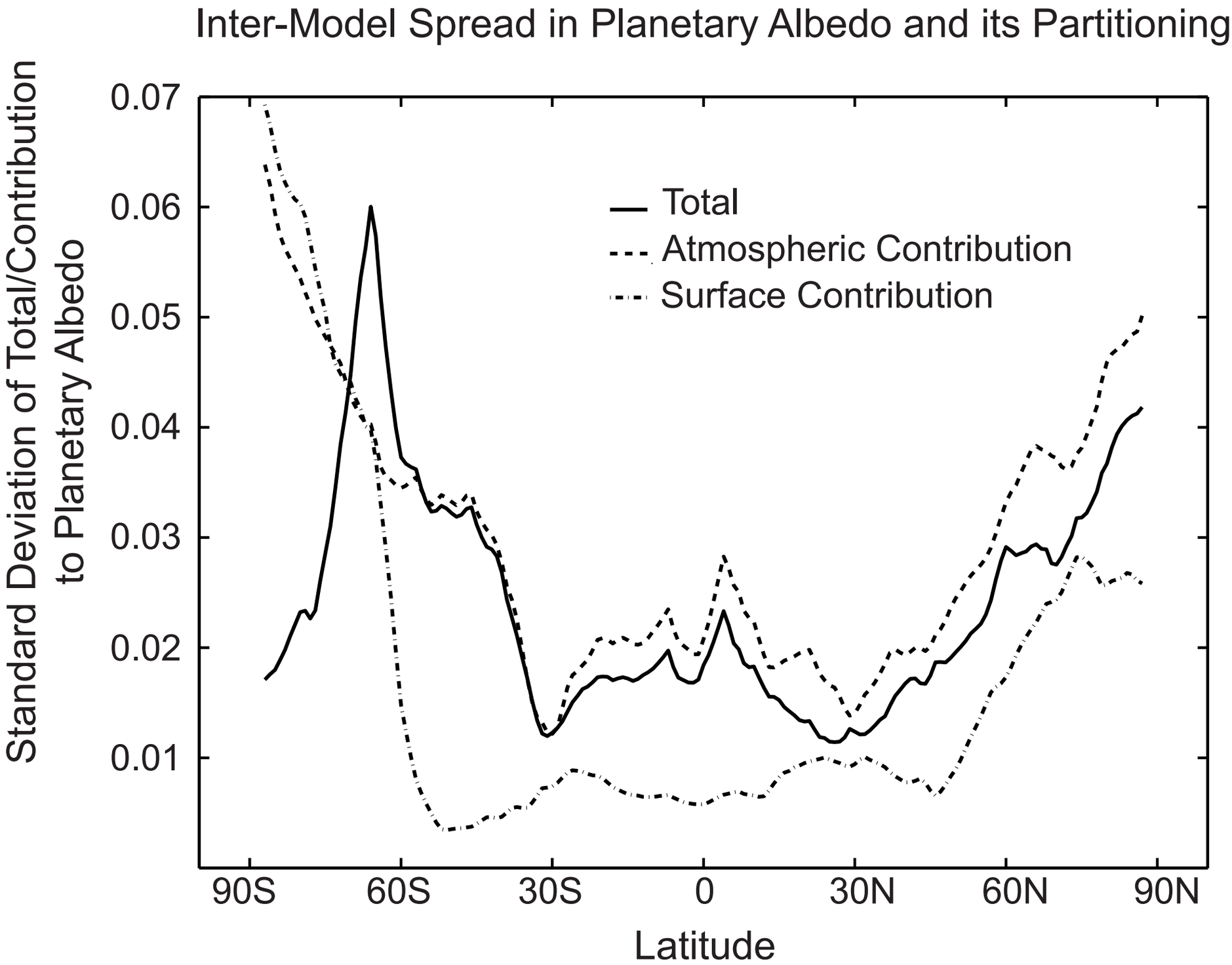

Figure 7. The inter-model standard deviation of zonal average planetary albedo (solid line), $\alpha_{P,ATMOS}$ (dashed line) and, $\alpha_{P,SURF}$ (dashed-dot line) for the CMIP3 PI simulations.

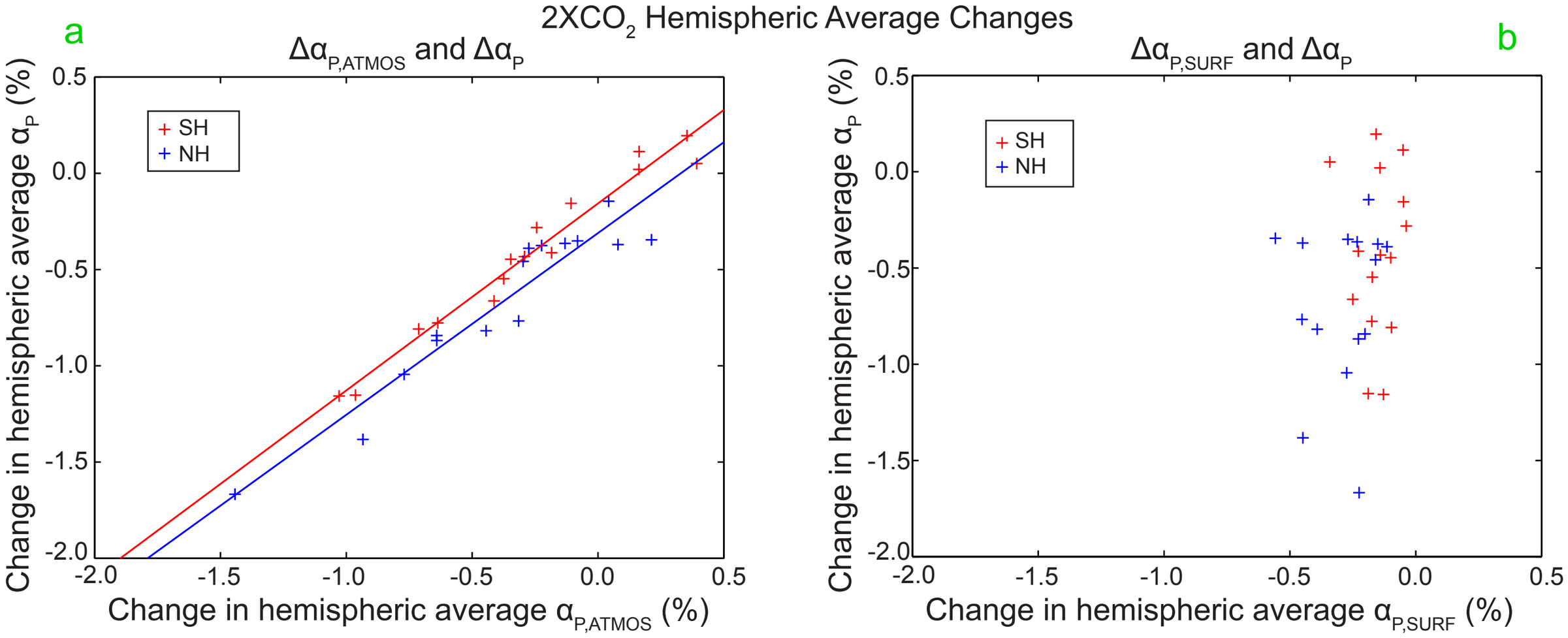

FIG 8. (a) Change in hemispheric average planetary albedo in the 2XCO2 runs (relative to the PI simulations) versus change in hemispheric average $\alpha_{P,ATMOS}$. The lines are the linear best fits in each hemisphere. (b) as in (a) except versus hemispheric average $\alpha_{P,SURF}$.

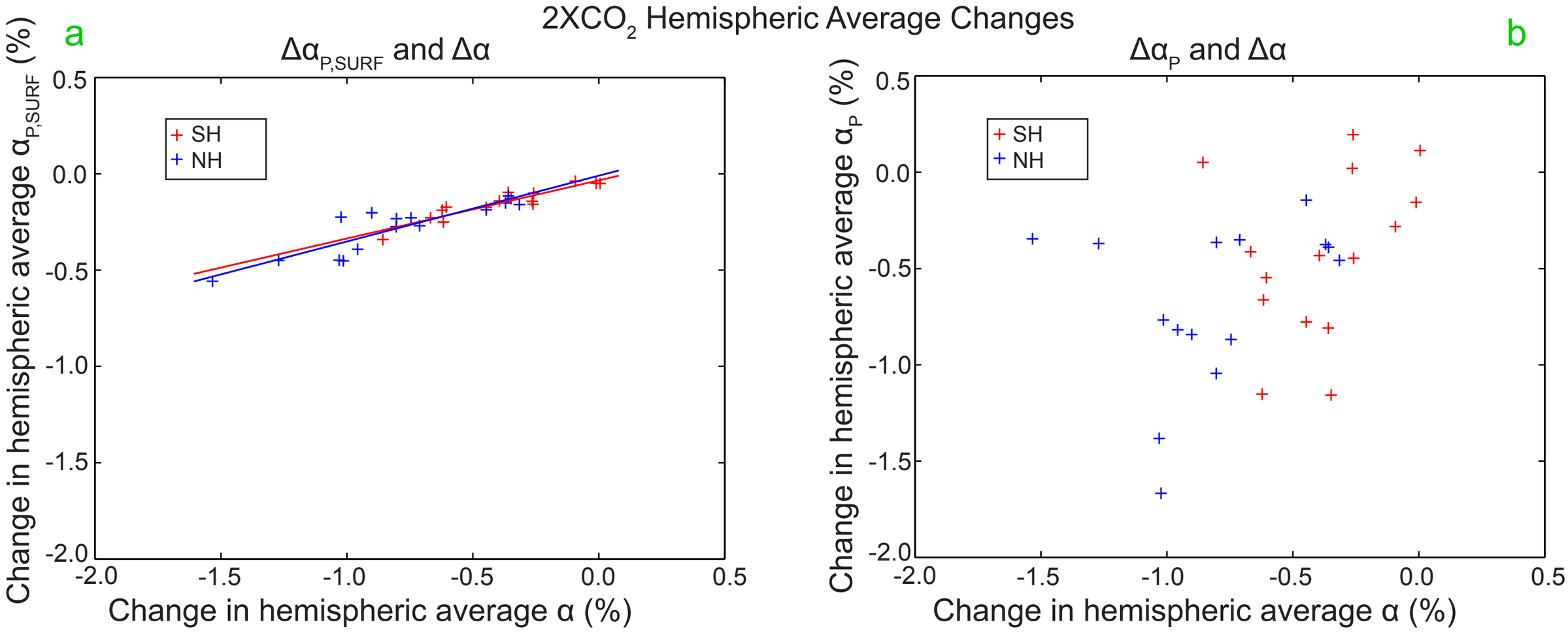

FIG 9. (a) Change in hemispheric average $\alpha_{P,SURF}$ in the 2XCO2 runs (relative to the PI simulations) versus change in hemispheric average surface albedo. The lines are the linear best fits in each hemisphere. (b) Change in hemispheric average planetary albedo in the 2XCO2 runs (relative to the PI simulations) versus change in hemispheric average surface albedo.

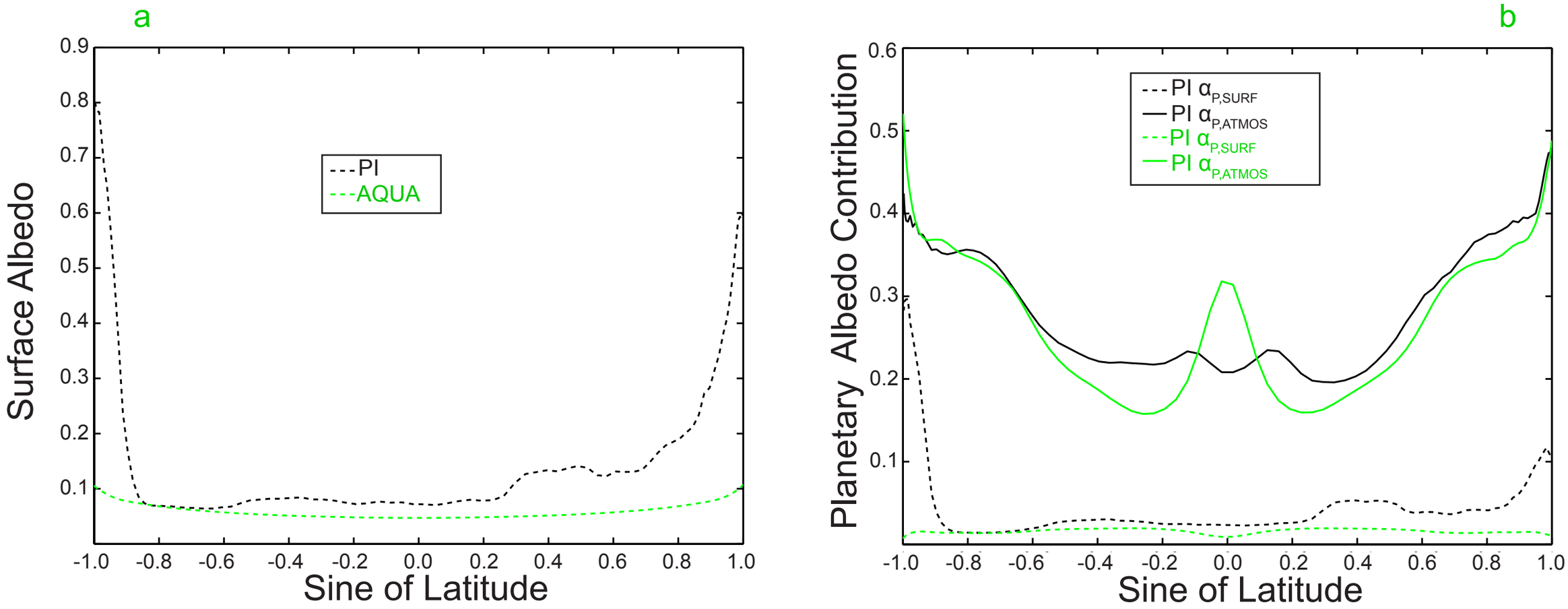

FIG 10. (a) Zonal average surface albedo in the GFDL simulations of the PI (black) and AQUA (green). (b) Zonal average $\alpha_{P,ATMOS}$, and $\alpha_{P,SURF}$ in the GFDL simulations of the PI (black) and AQUA (green). (c) and (d) as in (a) and (a) except for the NCAR simulations of the PI (black), QUAD (red), and LGM (blue).

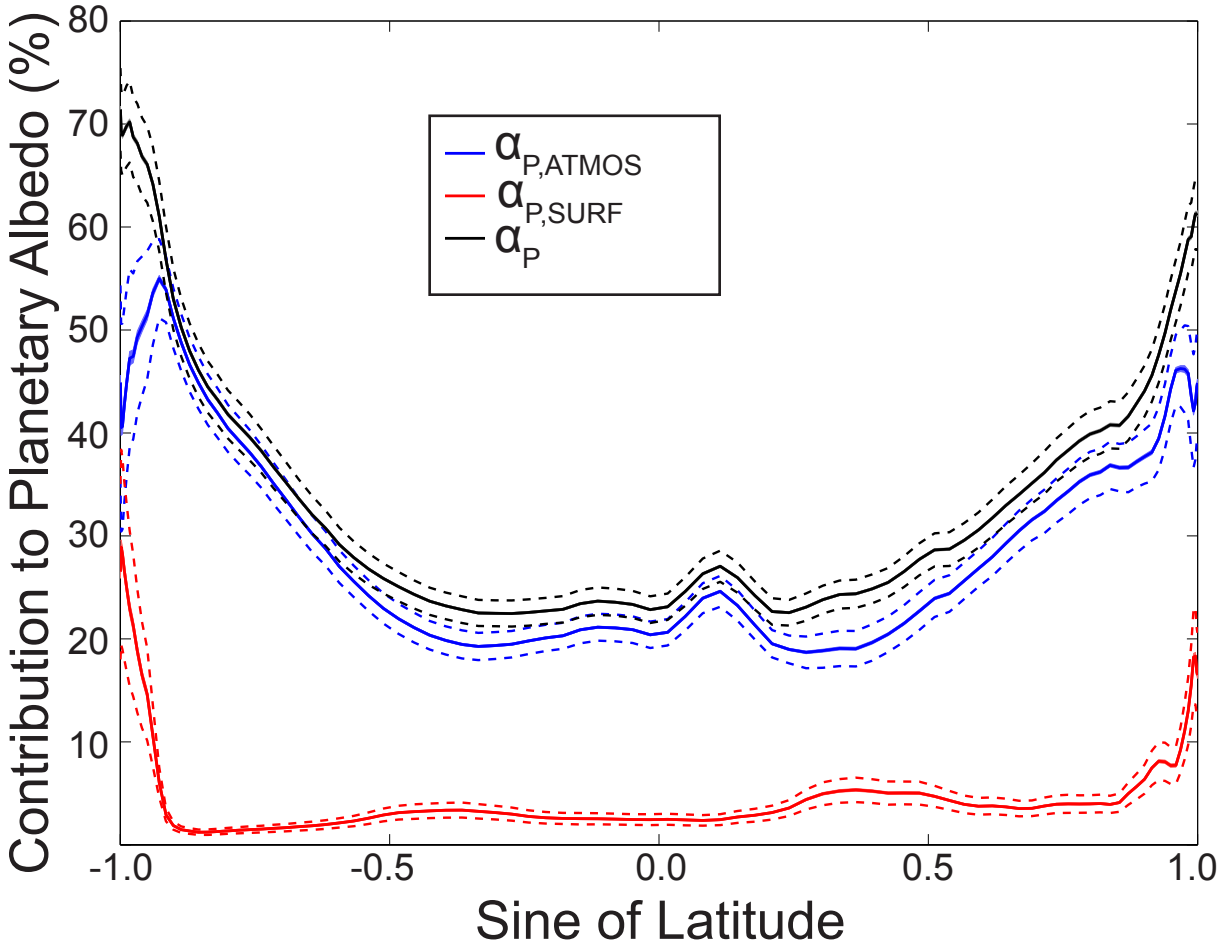

FIG A1. Zonal average planetary albedo, $\alpha_{P,ATMOS}$, $\alpha_{P,SURF}$, and $\alpha_{P,}$ calculated from the observations and their uncertainties (2σ) estimated from the Monte Carlo simulations described in the text. The shaded area is the uncertainty if the observational errors are random and uncorrelated at each gridpoint. The dashed lines are the uncertainty if the errors are systematic and perfectly correlated at all locations in each zonal band.

Observations

a

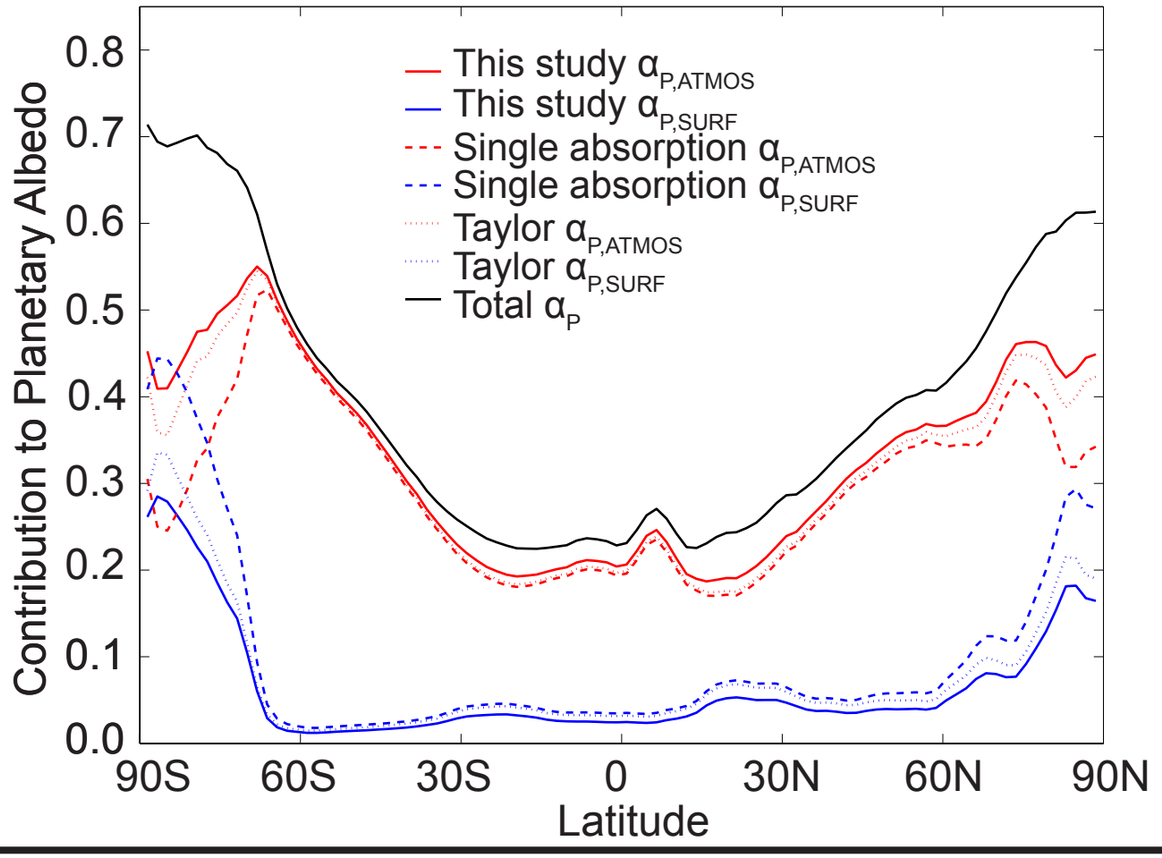

b

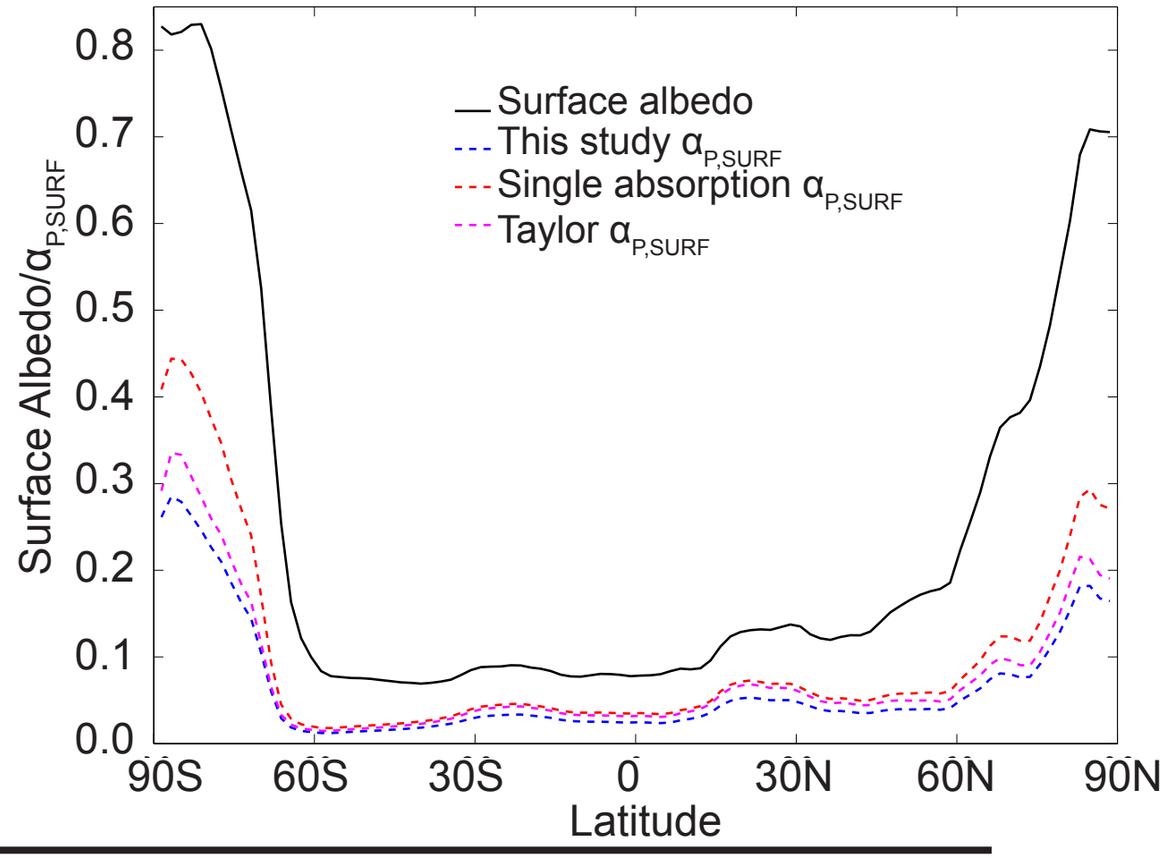

Inter-model Average

c

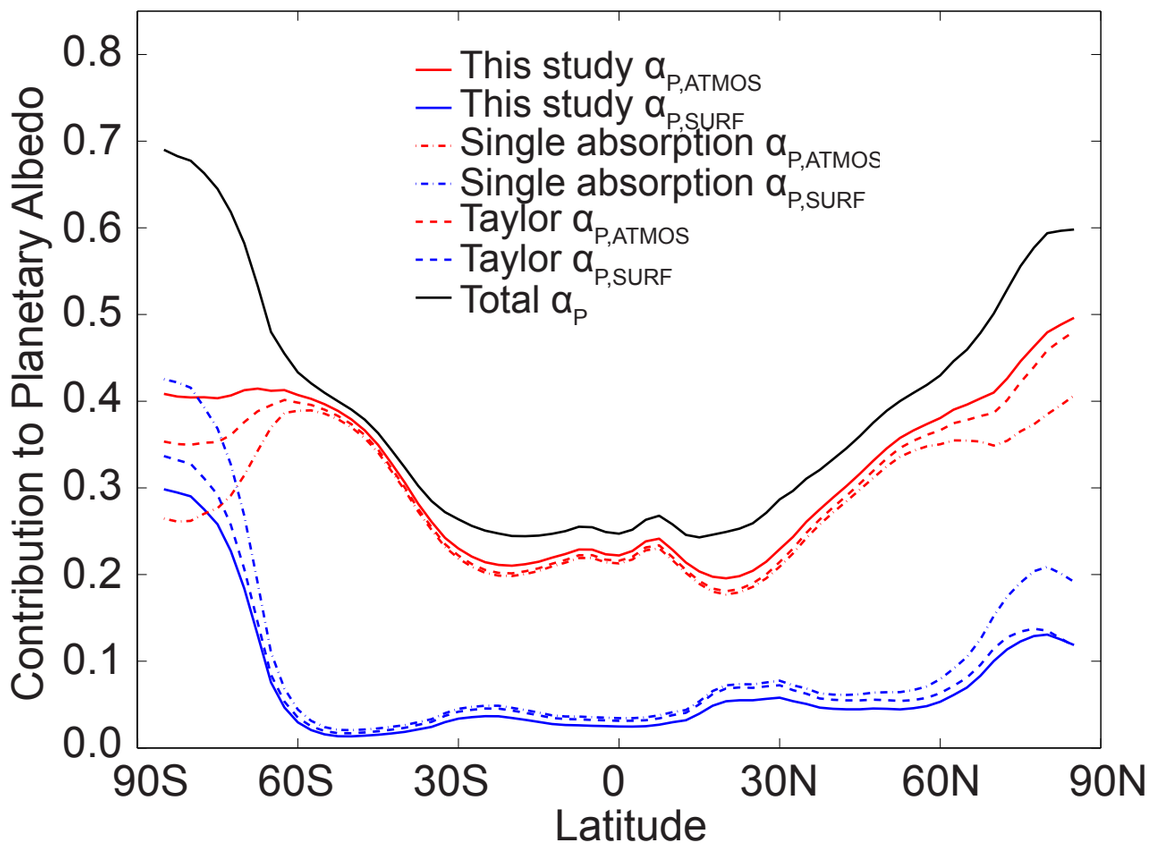

d